

Multi-phase Dynamic Modeling of Forest-to-Farm Transition and Sustainable Organic Agriculture

Enming Chu^{1, a*}, Yueyang Yin^{2, b} and Mengxi Song^{3, c}

¹School of Faculty of Electronic and Information Engineering, Xi'an Jiaotong University, Xi'an 710049, China;

²School of Management, Fudan University, Shanghai 200433, China.

³College of Integrated Circuits and Micro-Nano Electronics, Fudan University, Shanghai 200433, China.

^achuenmingwww@stu.xjtu.edu.cn, ^b22307130468@m.fudan.edu.cn, ^c22301030047@m.fudan.edu.cn

Abstract. We construct a dynamic model to explore the evolution of agroecosystems converted from forested areas, focusing on the key role of natural processes and human decisions. The process is divided into five stages: deforestation, initial agriculture, maturation of marginal habitats, ecosystem maturation, and organic agriculture transformation. In the deforestation stage, we calculated initial key data for the model such as soil nutrient content and weed biomass after deforestation. In the early stages of agriculture, we developed the Lotka-Volterra model and the Holling Type II model, which integrate crop, weed, insect, bird, and soil nutrient dynamics. By extending the traditional ecological models, we developed a coupled system of dynamic differential equations with multiple components incorporating events such as competition, predation, migration, seasonal sowing and harvesting, which were solved using a fourth-order Longe-Kuta method. Ablation experiments showed that cessation of herbicide use led to a 400% surge in weed biomass, which indirectly increased insect and bird populations by about 5% each, and led to a 100% surge in insect populations and a 200% increase in bird populations, which reduced the Ecosystem Stability Index (ESI). An earthworm-mediated soil-plant continuum model and a snake-mediated nutrient cascade dynamics model were introduced and constructed for the mature stage of marginal habitats. Simulation results showed that earthworms significantly increased soil nutrient content and crop growth by accelerating organic matter decomposition, while snakes negatively affected crop yield by influencing insect populations through bird predation. At the ecosystem maturity stage, herbicide deactivation resulted in a 66% decrease in yield and a significant reduction in ESI. To restore homeostasis, we introduced bats and nitrogen-fixing bacteria and compared them. Simulations showed that bats improved ecosystem stability and restored crop yields to 95% of their original levels. Nitrogen-fixing bacteria, although weaker overall, outperformed bats in localized soil restoration. Finally, the dual strategy of ecological prioritization and economic balance demonstrated complementary advantages in exploring paths of transformation in organic agriculture. The ecological priority model is suitable for ecologically fragile areas as it reduces soil erosion by 50 per cent and achieves a steady increase in yields through the implementation of crop rotation and cover crop cultivation. The Economic Balance model increases annual net income by about 12% through intercropping and precision agriculture and reduces fertilizer and pesticide use by 40-55%, despite a higher initial capital investment. Both models maintained ESI values above 0.9, indicating strong long-term sustainability. Based on these findings, we recommend the establishment of an Eco-Agriculture Transformation Fund to promote chemical-free agricultural practices.

Keywords: Ecosystem; Differential Equations; Lotka-Volterra Model; Holling II Model.

1. Introduction

The process of converting forests to farmland has far-reaching implications for ecological integrity and economic sustainability[1]. The loss of primary forests will accelerate the collapse of biodiversity, trigger soil degradation and pest outbreaks, forcing farmers to rely on chemical inputs to maintain yields, thus creating a vicious cycle, rising costs of agricultural production[2]. With gradual restoration of marginal habitats, reintroduction of native species can reduce reliance on chemical

inputs through natural pollination and pest suppression, thereby reducing economic expenditure and increasing ecosystem resilience[3]. However, the transition to organic agriculture requires a balance between short-term yield fluctuations and long-term economic-environmental synergies[4]. In this paper, we build a dynamic model to simulate the evolution of ecosystems after the conversion of forests to farmland, analyze the interactions between natural restoration mechanisms and human agricultural decisions. Our research plan and pathway as shown in Fig.1.

RQ1: Food web modeling in agroecosystems: construct dynamic model integrating crops, pests, natural predators and pesticide impacts to analyze effects on soil composition and biological chains.

RQ2: Impacts of native species re-emergence: modeling the ecological contributions of two reintroduced native species to agroecosystems.

RQ3: Herbicide removal: examine the competitive relationship between weeds and crops after herbicide removal. Analyze the dual pest control and pollination roles of bats in ecosystem stabilization and compare their impacts to another species.

RQ4: Organic agriculture trade-off assessment: Compare the long-term impacts of organic versus conventional agriculture in terms of pest management, soil health indicators and economic viability through a longitudinal analysis.

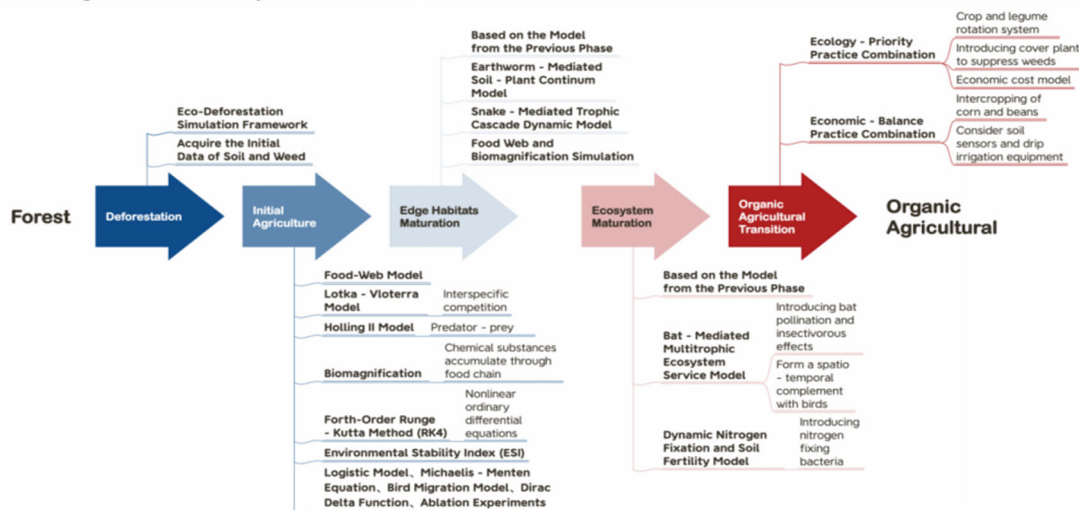


Fig. 1: The research plan and pathway of this paper

2. Dynamic Model of the Evolution of Agro-ecosystem Transition

2.1 Deforestation

Arable land is cleared from forests, so the initial soil nutrient content of arable land is divided into two parts, one is the undeforested forest, and the other is the original nutrients in the forested land, which is calculated by $S_{post} = S_0 \cdot (1 - E) + B_{residue} \cdot \delta$, where S_0 denotes the initial weed biomass, E is the erosion rate, $B_{residue}$ is the residual biomass, and δ represents the decomposition rate. The other part represents the weed biomass from decomposed residues. The initial biomass consists of the uncut portion as well as the plant residues after the cut portion, affecting crop cultivation, and is calculated by $V_{post} = V_0 \cdot (1 - D) + R \cdot V_0 \cdot D$, where V_0 is original nutrient content, D is the deforestation rate, and R represents the nutrient retention rate. These formulas describe the initial soil and weed conditions after converting forest to agricultural land.

2.2 Initial Agriculture: Model the Current Ecosystem

During the initial phase of forest conversion to agricultural ecosystems, the primordial state of the ecosystem exerts significant influence on subsequent agroecosystem establishment. In this Stage, We developed a multi-component coupled dynamic model to quantitatively analyze ecological succession processes following deforestation for cropland conversion. The framework integrates critical ecological interactions including crop-weed competition, insect and bird

population regulation, Bird migration, and soil nutrient cycling, while evaluating the stability impacts of herbicide and pesticide application.

2.2.1 Competition of Crops and Weeds

The Lotka-Volterra model[5] employs differential equations to characterize interspecific resource dynamic competition, with its development proceeding through three distinct phase.

Single-Species Growth Model: Assuming the instantaneous growth rate of a species depends solely on its population density, i.e., $dN/dt=rN$ where r is the intrinsic growth rate and N is population size.

Environmental Carrying Capacity Constraint (Logistic Model): The environmental carrying capacity K represents the maximum sustainable population size. Under such assumption, The modified equation becomes: $dN/dt=rN(1-N/K)$ where population growth ceases 0 as N approaches K .

Two-Species Competition Model: For crops (C) and weeds (W) sharing resources, mutual growth inhibition is quantified by competition coefficients α_{ij} :

$$\frac{dC}{dt}=r_c C \left(1-\frac{C+\alpha_{cW}W}{K_c}\right) \quad \frac{dW}{dt}=r_w W \left(1-\frac{W+\alpha_{wC}C}{K_w}\right)$$

There are two possible scenarios. When $dC/dt = 0$ intersects $dW/dt = 0$ in the first quadrant, the two species are said to coexist stably. Trajectories starting from different initial conditions will eventually tend towards the stable coexistence point. This indicates that regardless of the initial quantities of C and W , in the long-term evolutionary process. When $dC/dt = 0$ and $dW/dt = 0$ have no intersection in the first quadrant, the two species are said to be in competitive exclusion.

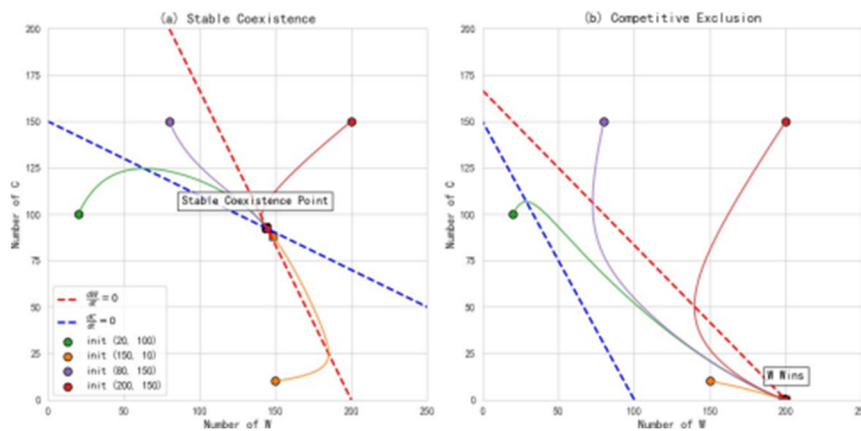


Figure 2: Two possible state of crop and weed

However, traditional Lotka-Volterra models do not consider the effects of human activities and biological regulation, and its simplified assumptions (such as unlimited resources and constant environment) cannot portray the complexity of the agricultural ecosystem.

Nutrient-Limited Michaelis-Menten Kinetics: Plant growth is regulated by soil nutrient concentration N , modeled using Michaelis-Menten kinetics:

$$G(N)=\frac{N}{N+K_N}$$

where K_N represents the half-saturation constant, reflecting crop nutrient sensitivity. When $N \ll K_N$, growth rates decline significantly, simulating productivity suppression under nutrient-poor conditions.

Selective Suppression of Herbicides: Herbicide (H) regulates competitive balance through photosynthetic inhibition of weeds:

$$\frac{dC}{dt} \propto (1-\eta_{HC}H) \quad \frac{dW}{dt} \propto (1-\eta_{HW}H)$$

The model quantifies this effect through ηHW , and crops are only weakly affected due to their herbicide-resistant traits (ηHC is extremely small). Note: $H = 0$ during winter.

Insect Consumption: Crop consumption by insects follows Holling Type II functional response model[6], which is mathematically expressed as:

$$a_c = \frac{t_c C}{1 + h_c t_c C}$$

where a_c represents crop biomass consumed by insects per unit area and time; t_c quantifies maximum search efficiency at low crop densities; h_c denotes average duration required to process unit crop biomass. The amount of plant is completely sufficient for insects, so it can be seen as in the saturation stage, that is:

$$a_c = \frac{1}{h_c} \quad a_w = \frac{1}{h_w}$$

Event-Driven Sowing-Harvesting Model: Crop biomass follows agricultural cycle constraints, so we assume that farmers sow in March and harvest in September each year. We introduce **Dirac delta function** $\delta_{harvest}$ to describe the harvesting event:

$$\delta_{harvest} = \begin{cases} 0 & t \neq n + 0.75 \\ 1 & t = n + 0.75 \end{cases}$$

with n denoting years and time standardization $t \in [0, 1]$ corresponds to the natural year. Harvesting removes all the biomass. By the same method, we introduce δ_{sow} to describe the sowing event:

$$\delta_{sow} = \begin{cases} 0 & t \neq n + 0.25 \\ 1 & t = n + 0.25 \end{cases}$$

Sowing event expression is $\delta \cdot C_{sow}$ with C_{sow} corresponds to the biomass of sowing every year.

Integrated Differential System: Based on the above mechanism, the dynamic changes of crops and weeds are described by the following equations:

$$\begin{aligned} \frac{dC}{dt} &= r_c \cdot C \cdot \left(1 - \frac{C + a_{cW} W}{K_c} \right) \cdot \frac{N}{N + K_N} - a_c I C - (1 - \eta_{HC}) \cdot H \cdot C - \delta_{harvest} \cdot C + \delta_{sow} \cdot C_{sow} \\ \frac{dW}{dt} &= r_w \cdot W \cdot \left(1 - \frac{W + a_{wC} C}{K_w} \right) \cdot \frac{N}{N + K_N} - a_w I W - (1 - \eta_{HW}) \cdot H \cdot W \end{aligned}$$

2.2.2 Insect Population Dynamics

Insect populations act as primary consumers in the agricultural ecosystem. Building upon the crop-weed competition framework in 2.1.1, we develop a dynamic model integrating Holling Type II functional responses. Insect growth depends on crop (C) and weed (W) biomass, which serve as their primary food sources. Following the Lotka-Volterra predator-prey framework, the intrinsic growth rate is proportional to plant biomass:

$$\frac{dI}{dt} = \beta \cdot (C + W) \cdot I - d_I \cdot I$$

where β represents the insect reproductive efficiency coefficient, and d_I denotes natural mortality. This formulation assumes linear scaling between plant biomass and insect reproduction, valid under non-limiting nutrient conditions.

Pesticide (P) amplify insect mortality through neurotoxic and metabolic disruptions. We model this as an additive mortality term $\eta_p \cdot P \cdot I$, where η_p quantifies the pesticide's lethality. Note: $P = 0$ during winter.

In the **food-web bioaccumulation model**[7], biomagnification stands as one of the most critical fundamental principles. This effect causes the fugacity and concentration of chemicals to increase with rising trophic levels. To quantify herbicide (H) impacts on insect mortality via trophic transfer, we introduce a delayed cumulative exposure mechanism:

$$H_I(t) = \int_{t-\tau_1}^{t-\tau_2} \zeta_{HI} \cdot H(s) \cdot e^{-\phi_{HI}(t-s)} ds$$

where $H(s)$ is time-dependent herbicide application intensity; τ_1, τ_2 is exposure memory window ($\tau_2 < \tau_1$ represents delayed biomagnification); ζ_{HI} is conversion coefficient of herbicides; ϕ_{HI} is Metabolic elimination rate of herbicide in insects; $e^{-\phi_{HI}(t-s)}$ is physiological decay factor for metabolic processes. Additionally, birds (B) regulate insect populations via density-dependent predation. Adopting the above Holling Type II model. Combining these mechanisms yields the full insect dynamics equation:

$$\frac{dI}{dt} = \beta \cdot (C+W) \cdot I - \gamma_B \cdot B \cdot I - (d_I + \eta_P P + H_I) \cdot I$$

2.2.3 Bird Migration and Predation

As secondary consumers in the agricultural ecosystem, birds play dual roles as insect predators and migratory species. Their dynamics are governed by three key mechanisms: (1) seasonal migration patterns driven by photoperiodic cues, (2) energy acquisition through Holling Type II predation on insects, and (3) pesticide-induced mortality through trophic transfer. The model integrates these components through coupled differential equations, extending the insect population framework described in 2.1.2. Bird migration follows periodic patterns aligned with agricultural seasons. We employ a cosine function to model population flux: $m_B(t) = \cos(2\pi t)$ where t represents normalized annual time ($t=0$: January 1st). This formulation generates peak influx during March ($t=0.25$) when insect populations reach maximum density, aligning migratory behavior with resource availability. Following the biomagnification framework, we model cumulative pesticide exposure:

$$P_B(t) = \int_{t-\tau_1}^{t-\tau_2} \zeta_{PB} \cdot P(s) \cdot e^{-\phi_{PB}(t-s)} ds$$

The cumulative herbicide exposure in birds follows delayed integrator dynamics:

$$H_B(t) = \int_{t-\tau_1}^{t-\tau_2} \zeta_{HB} \cdot H(s) \cdot e^{-\phi_{HB}(t-s)} ds$$

The bird population equation incorporates energy conversion, mortality, and migration:

$$\frac{dB}{dt} = \epsilon \cdot \gamma_B \cdot B \cdot I - (d_B + H_B + P_B) \cdot B + m_B(t) \cdot B$$

where $\epsilon = 0.1$ represents energy conversion efficiency from prey biomass. The system couples with insect dynamics through the $\gamma_B \cdot B \cdot I$ term in equation 21, creating predator-prey feedback loops.

2.2.4 Soil nutrient cycle

The soil nutrient cycle serves as the foundation for agricultural productivity and ecosystem stability. Building upon the crop-weed competition framework and predator-prey dynamics, we develop a mechanistic model integrating microbial decomposition, fertilization practices, and erosion processes. This subsystem directly links plant growth dynamics with human agricultural management through bidirectional feedback mechanisms. Human fertilization practices follow seasonal patterns synchronized with planting cycles, where F_0 represents fertilization amount:

$$F(t) = \begin{cases} F_0 \cdot N & t \in [n+0.25, n+0.75] \\ 0 & \text{else} \end{cases}$$

The differential equation governing soil nutrient concentration N is:

$$\frac{dN}{dt} = \delta \cdot (\rho_C \cdot C + \rho_W \cdot W) - \alpha \cdot (C+W) \cdot \frac{N}{N+K_N} - E \cdot N + F(t)$$

2.2.5 Solution of the Model

We employ the **fourth-order Runge-Kutta method (RK4)**. To apply the RK4 method, we discretize the time domain into small intervals with a time step of $h = 0.01$ years (approximately

3.65 days). The iterative process was repeated for 500 time steps, corresponding to the 5-year simulation period, and got the results.

$$y_{t+1} = y_t + \frac{1}{6}(k_1 + 2k_2 + 2k_3 + k_4)$$

As shown in Figure 3(a), in the first-year of the application of herbicides, the biomass of weeds drops sharply, and continuous application leads to a gradual decrease. Figure 3(b) shows that weeds exert competitive pressure on crops through mechanisms. Meanwhile, the non-use of pesticides leads to serious damage to crops. Yield analysis shows that the combined use of herbicides and pesticides results in the highest yield. Figure 3(c) shows that in the early planting stage, herbicides have a weak impact on insects, while pesticides cause a significant reduction in insect populations. Herbicides then indirectly affect insect dynamics. Among them, pesticides have a more significant impact. In addition, the biomagnification of chemical substances in birds also contributes to the decline in their numbers. In terms of soil nutrients, as shown in Figure 3(e), herbicides directly affect soil organic matter. Pesticides, on the other hand, change the soil nutrient cycling through different ecological mechanisms.

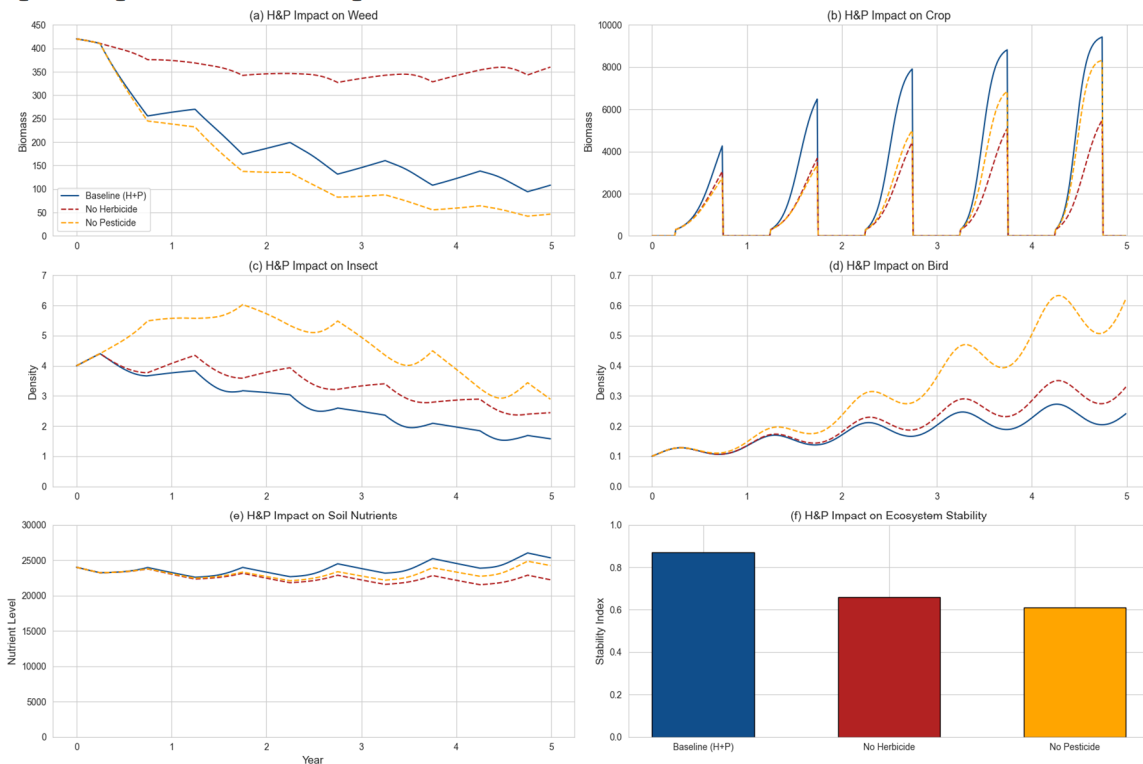


Figure 3: Results of task 1

To quantify the overall stability of the agricultural ecosystem under different agrochemical usage scenarios, we developed the **Environmental Stability Index (ESI)**. The ESI is formulated as: $ESI = w_1 \cdot \text{Soil Quality} + w_2 \cdot \text{Pest Control} + w_3 \cdot \text{Crop Health}$, where w_1 , w_2 , and w_3 are weighting coefficients that reflect the relative importance of each component.

Soil quality was evaluated through the quantification of soil organic matter (SOM) content.

$$\text{Soil Quality} = \frac{SOM_{\text{observed}}}{SOM_{\text{MAX}}}$$

where SOM_{observed} represents the field-measured organic matter content, and SOM_{max} denotes the theoretical maximum achievable under ideal pedological conditions.

The ecosystem's pest regulation capacity was characterized by the dynamic equilibrium between herbivorous insect populations (P) and their avian/chiropteran predators (B).

$$\text{PestControl} = 1 - \frac{P}{P+k \cdot B}$$

incorporates three key parameters: P (pest biomass density), B (predator biomass), and k , a dimensionless scaling factor representing predator foraging efficiency.

Crop health assessment focused on yield realization relative to agroecological potential:

$$CropHealth = \frac{Y_{actual}}{Y_{potential}}$$

where Y_{actual} corresponds to measured crop yields, while $Y_{potential}$ represents the theoretical maximum yield achievable under optimal nutrient availability and complete pest exclusion.

As shown in Figure 3(f), scenarios with combined herbicide and pesticide use achieved the highest ESI(0.87), indicating superior short-term stability. However, longitudinal simulations revealed diminishing returns in soil quality under prolonged chemical use.

2.3 Edge Habitat Maturation: Incorporate the Reemergence of Species

Native species gradually reestablish in the agricultural ecosystem, altering its dynamics through trophic interactions. We extend the baseline model (Section 2.2) by incorporating two species: earthworms ($Worm$) as decomposers and snakes (S) as tertiary consumers. The inclusion of earthworms establishes a critical decomposition pathway, linking plant residues to soil nutrient pools, while snakes introduce apex predation pressure that cascades through lower trophic levels.

Earthworms enhance soil fertility by accelerating organic matter decomposition and improving soil structure. Their biomass ($Worm$) is governed by logistic growth, predation pressure from birds, and natural mortality, where d_W quantifies the soil enhancement factor from earthworm activity.

$$\frac{dWorm}{dt} = r_{Worm} \cdot Worm \cdot \left(1 - \frac{Worm}{K_{Worm}}\right) - (d_{Worm} + \gamma_B \cdot B) \cdot Worm$$

$$\frac{dN}{dt} = \delta \cdot (\rho_C \cdot C + \rho_W \cdot W) \cdot (1 + d_W \cdot Worm) - \alpha \cdot (C + W) \cdot \frac{N}{N + K_N} - E \cdot N + F(t)$$

Snakes act as apex predators, regulating bird populations through density-dependent predation.

$$\frac{dS}{dt} = \epsilon \cdot \gamma_S \cdot S \cdot B - (d_S + H_S + P_S) \cdot S$$

$$\frac{dB}{dt} = \epsilon \cdot \gamma_B \cdot B \cdot (I + Worm) - (d_B + \gamma_S \cdot S + H_B + P_B) \cdot B + m_B(t) \cdot B$$

where γ_S is the snake predation efficiency on birds, d_S the natural mortality rate, P_S the cumulative herbicide exposure and P_B the cumulative pesticide exposure.

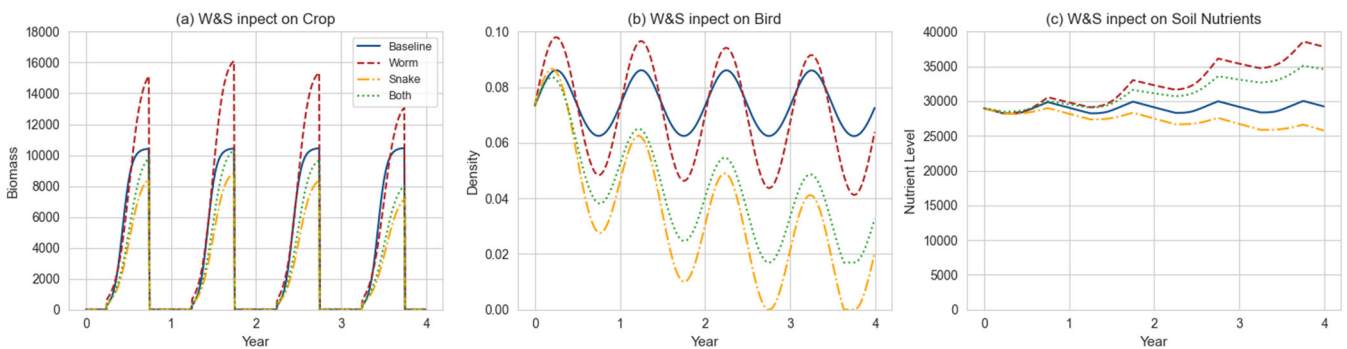


Figure 4: Results of task 2

Figure 4(a) shows the biomass of crops. When only earthworms return, they loosen the soil and accelerate the decomposition of organic matter, resulting in the largest increase in biomass. After snakes return, they prey on birds, indirectly causing insect pests. When earthworms and snakes act together, the negative effects outweigh the positive effects of earthworms, and the total biomass decreases. Figure 4(b) presents the change in the biomass of birds. When earthworms return, the amount of crops and weeds increases, providing abundant food for birds. The biomass fluctuates significantly with the migration cycle. Figure 4(c) shows the change in the organic matter content of the land. The return of earthworms has the most direct and significant effect.

2.4 Ecosystem Maturation

2.4.1 Removal of Herbicide

After discontinuing the use of herbicides, the number of weeds will show an upward trend. The large-scale growth of weeds not only encroaches on the growing space of crops, competes for the nutrients that should be supplied to crops, but also provides a breeding and inhabiting place for pests. Under the dual influence of weed growth and pest reproduction, the biomass of crops drops to one-third of that when herbicides were used (Figure 5).

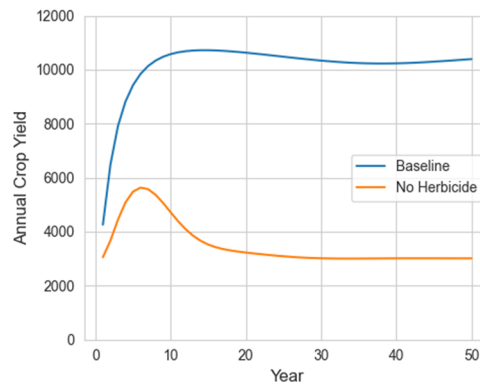


Figure 5: Comparison of the impacts of herbicide use or non-use on the annual crop yield

By simulating and calculating the environmental stability index of the farm environment, it is found that this index has dropped from the original 0.87 to 0.36, with a decrease of approximately 59% (Figure 3). It can be inferred from this that stopping the use of herbicides has significantly damaged the environmental balance of cultivated land.

2.4.2 Incorporating Bats into the Food Web Model

To make up for the damage to the environmental balance, bats are introduced into the cultivated land. Bats can prey on pests in the ecosystem. Their ecological niche is similar to that of birds. In addition to preying on pests, they also have the function of assisting in crop pollination. The ecological services and competitive effects of bats (B_{Bat}) are quantified through a **four-equation system: Pollination Effect, Pest Predation, Interspecific Competition, and Bat Population Dynamics:**

$$\begin{aligned} \frac{dC}{dt} &= \left(r_c \cdot C \cdot \left(1 - \frac{C + \alpha_{CW} W}{K_C} \right) + \varphi \cdot Bat \right) \cdot \frac{N}{N + K_N} - a_c I C - \delta_{harvest} \cdot C + \delta_{sow} \cdot C_0 \\ \frac{dI}{dt} &= \beta \cdot (C + W) \cdot I - \gamma_B \cdot B \cdot I - \mu_{Bat} \cdot Bat \cdot I - d_I \cdot I \\ \frac{dB}{dt} &= \epsilon \cdot \gamma_B \cdot B \cdot I - (d_B + \alpha_{BB}) \cdot B + m_B(t) \cdot B \\ \frac{dBat}{dt} &= \epsilon \cdot \mu_{Bat} \cdot Bat \cdot I - \alpha_{BB} \cdot Bat \cdot B - d_{Bat} \cdot Bat \end{aligned}$$

where φ is the pollination efficiency coefficient, μ_{Bat} is the bat predation rate. Its nocturnal activity characteristics form a **spatio-temporal complement** with those of birds (B). α_{BB} is the competition coefficient, reflecting the degree of overlap in diet and habitat. d_{Bat} represents the natural mortality rate.

After the introduction of bats, significant changes have occurred in the farmland ecosystem. The crop biomass increased by 35% in the first year after the introduction of bats. By the fourth year, it had recovered to 95% of the level before the discontinuation of herbicides.

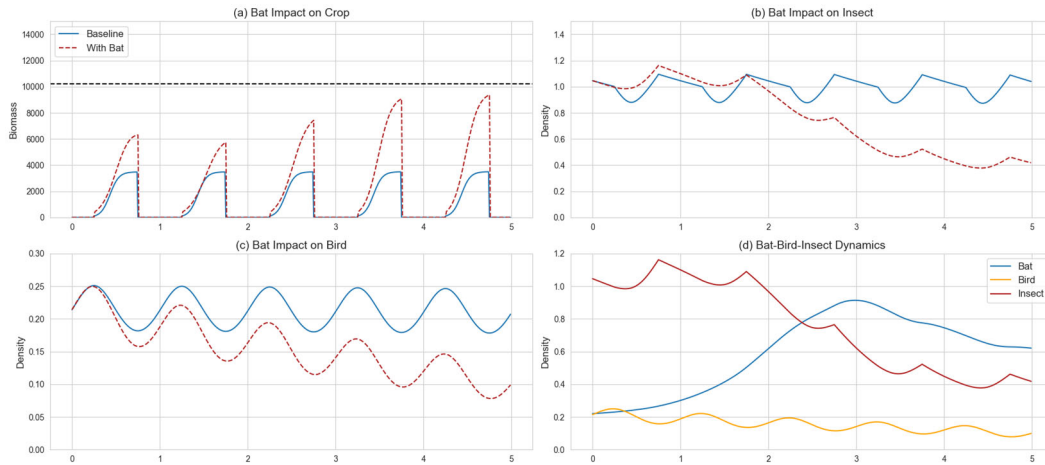


Figure 6: The results after introducing bats

Among them, the pollination effect contributed 60% of the increase. The pest biomass decreased by 50% in the first year and stabilized at 20% of the original value. Moreover, although the bird biomass decreased by 12%, the feeding efficiency per individual increased, and the bird population did not collapse, maintaining the stability of the ecosystem. After 5 years, the environmental stability index rebounded from 0.36 to 0.78, indicating that the stability of the ecosystem has been restored.

After that, an attempt was made to introduce nitrogen-fixing bacteria for comparison. Nitrogenfixing bacteria are a type of bacteria living in the soil. They can convert the free nitrogen in the air, which cannot be absorbed by plants. The modeling of nitrogen-fixing bacteria is as follows:

$$\frac{dN_{fix}}{dt} = r_{fix} \cdot N_{fix} \cdot \left(1 - \frac{N_{fix}}{K_{fix}}\right) - \mu_N \cdot W \cdot N_{fix}$$

which describes nitrogen-fixing bacterial population dynamics. Here, r_{fix} and K_{fix} represent the bacterial growth rate and carrying capacity, respectively, while μ_N characterizes the inhibitory effect of weeds on bacterial proliferation through resource competition.

In the farmland ecosystem, the bat model and the nitrogen-fixing bacteria model show different ecological effects. In terms of crop restoration, the crop biomass in the bat model recovered to 95% after 4 years, while the nitrogen-fixing bacteria model only took 3 years to recover to 85%. In terms of soil restoration, nitrogen-fixing bacteria can increase the soil nitrogen content by a significant 180%, while the bat model has no direct effect. This indicates that the two models have their own advantages in different ecological indicators, providing different strategic references.

Table 1: Results of task 4

Variables	Crop Biomass	Pest Biomass	ESI
After Stopping Herbicide Use (Initial)	33%	320%	0.36
4th Year after Bat Introduction	95%	20%	0.78
4th Year after Nitrogen-fixing Bacteria Introduction	85%	80%	0.65

2.5 Organic Agriculture Transition: Go Green

Building upon the matured agricultural ecosystem, we explore the transition to organic farming with two strategic models: ecological-priority practices and economic-ecological balance practices.

2.5.1 Ecological-Priority Strategy (Crop Rotation + Cover Crops)

Rotating crops with nitrogen-fixing legumes naturally replenishes soil nitrogen through symbiotic root bacteria, while breaking pest cycles and balancing nutrient demands. Cover crops

protect against erosion, suppress weeds, reducing synthetic fertilizer dependency. The dynamic equations extend the baseline Lotka-Volterra competition model:

1. Cover crop dynamics:

(1) Non-planting season:

$$\frac{dW_{cover}}{dt} = r_{cover} \cdot W_{cover} \cdot \left(1 - \frac{W_{cover}}{K_{cover}}\right) \cdot \frac{N}{N+K_N} - a_{W_{cover}} \cdot W_{cover} - \delta_{harvest_c} \cdot W_{cover} + \delta_{sow_c} \cdot W_{sow}$$

(2) Planting season: $\frac{dW_{cover}}{dt} = 0$

Cover crop biomass W_{cover} is modeled using logistic growth during non-planting seasons (September–February), with growth rate r_{cover} and carrying capacity K_{cover} kg/m².

2. Crop dynamics equations for the impact of additional crop rotations

(1) Conventional crop year:

$$\frac{dC}{dt} = r_C \cdot C \cdot \left(1 - \frac{C + \alpha_{CW} W}{K_C}\right) \cdot \frac{N}{N+K_N} - a_C \cdot C - \delta_{harvest} \cdot C + \delta_{sow} \cdot C_{sow}$$

(2) Legume crop year:

$$\frac{dC}{dt} = r_C \cdot C \cdot \left(1 - \frac{C + \alpha_{CW} W}{K_C}\right) \cdot \frac{N}{N+K_N} - a_{C_{legume}} \cdot C - \delta_{harvest} \cdot C + \delta_{sow} \cdot C_{sow}$$

$$\frac{dN}{dt} = \delta \cdot (\rho_C \cdot C + \rho_W \cdot W + \rho_{W_{cover}} \cdot W_{cover}) - a \cdot (C+W) \cdot \frac{N}{N+K_N} - E \cdot N + F(t)$$

A triennial rotation cycle alternates conventional crops (r_C) and legumes ($r_{C_{legume}}$). Legumes enhance nitrogen fixation, so in legume crop years, introducing an additional nutrient input term ($+0.1 \cdot C$) in plant decomposition items of soil dynamics (Equation 53).

3. Equations for weed dynamics under cover crop competition

$$\frac{dW}{dt} = r_W \cdot W \cdot \left(1 - \frac{C+W + \alpha_{WW} W_{cover}}{K_W}\right) \cdot \frac{N}{N+K_N} - a_W \cdot W$$

Cover crops occupy spatial resources, modifying weed competition to include a suppression term $\rho_{W_{cover}}$ in the weed growth equation.

Two key aspects of the rotation logic are crop type switching and time event adjustment. In terms of time-event adjustment, the crop type parameter is switched according to the crop rotation cycle at planting time in March each year.

2.5.2 Economic Balance Strategy (Intercropping + Precision Agriculture)

Intercropping, the practice of growing multiple crops on the same land simultaneously, enhances land use efficiency and promotes complementary benefits among crops. Precision agriculture leverages modern information technology to accurately manage farmland resources through real-time monitoring and adjustment of water and fertilizer application.

1. Crop dynamics equation:

$$\frac{dC_A}{dt} = r_A \cdot C_A \cdot \left(1 - \frac{C_A + C_B + \alpha_{CAW} W}{K_C}\right) \cdot \frac{N}{N+K_N} - a_{C_A} \cdot C_A - \delta_{harvest} \cdot C_A + \delta_{sow} \cdot C_{sow_A}$$

$$\frac{dC_B}{dt} = r_B \cdot C_B \cdot \left(1 - \frac{C_A + C_B + \alpha_{CBW} W}{K_C}\right) \cdot \frac{N}{N+K_N} - a_{C_B} \cdot C_B - \delta_{harvest} \cdot C_B + \delta_{sow} \cdot C_{sow_B}$$

Crop species C_A and C_B compete via a shared carrying capacity K_C , with interspecific competition coefficient α_{CAW} and α_{CBW} .

2. Soil nutrient dynamic equations

$$F(t) = F_0 \cdot r_{\text{sensor}} \cdot \left(1 - \frac{N}{N_{\text{target}}}\right) \qquad P(t) = P_0 \cdot r_{\text{sensor}} \cdot \frac{I}{I_{\text{threshold}}}$$

Dynamic herbicide use: $H(t) = H_0 \cdot r_{\text{sensor}} \cdot \frac{W}{W_{\text{threshold}}}$

Fertilizer ($F(t)$), pesticide ($P(t)$) and herbicide ($H(t)$) applications are dynamically adjusted using sensor data. N_{target} is the target soil nutrient level and the sensor accuracy vector r_{sensor} affects the fertiliser application efficiency.

3. Economic cost model

Consider the following total cost equation:

$$\text{Cost} = \int_0^T \left(C_{\text{tech}} + C_{\text{fertilizer}} \cdot F(t) + C_{\text{pesticide}} \cdot P(t) + C_{\text{herbicide}} \cdot H(t) \right) dt$$

$$\text{Revenue} = \int_0^T \left(P_A \cdot C_A + P_B \cdot C_B \right) dt$$

Total costs integrate technology investments C_{tech} , fertilizer $C_{\text{fertilizer}}$, and pesticide $C_{\text{pesticide}}$ expenses. Revenue depends on crop prices P_A and P_B .

Based on the baseline scenario in the second stage, the model introduces intercropping and precision resource management strategies, and analyses the changes in total crop yield, resource use efficiency, soil health and economic costs over a 30-year simulation cycle.

2.5.3 Comparison of the impacts of two organic farming combinations

Table 2: Comparison of indicators between ecology-prioritized and economic-balance models

Indicator	Ecology-prioritized Model	Economic-Balance Model
Soil nutrient level	+12%	+15%
Soil erosion rate	-50%	0%
Crop yield	-8% → 0%	+18%
Insect density	+20% → 0%	+10%
Bird density	+40%	+25%
Fertilizer use	0%	-40%
Pesticide use	-100%	-55%
Economic net return	0%	+12%
Technology cost	0\$/m ²	0.2\$/m ²
ESI	0.94	0.91

In summary, the ecology-priority model focuses on restoration, while the economic-balance one integrates ecological and economic benefits. Both strategies have a 10% higher ESI than before, indicating greater sustainability.

3. Sensitive Analysis

We categorized parameters in this paper into two categories: natural constants and adjustable parameters. Nine representative parameters were selected for sensitivity analysis. The specific analysis results are shown in Table 3.

Table 3: Sensitivity analysis results for key parameters

Parameter Type	Parameter Symbol	Class ($ \Delta \text{ESI} $)
Variable Parameter	η_{HW}, η_P	High (>0.05)
	m_W	Medium (0.01 0.05)
	$Worm_0$	Low (<0.01)
Natural Constant	K_C, K_W	High (>0.05)

r_C, r_W
 d_I

Medium (0.01 0.05)
Low (<0.01)

From the data in Table 3, it can be observed that among the adjustable parameters, η_P (additional mortality rate of insects caused by pesticides) and η_{HW} (inhibition rate of herbicides on weeds) exhibit high sensitivity. This finding suggests that although chemical interventions can effectively control pest and weed populations in the short term, excessive reliance on such methods may lead to a decline in ecosystem resilience over time. Further experimental validation and data analysis are required to ensure the reliability and accuracy of the model results.

4. Model Evaluation and Further Discussion

Highly Comprehensive Model with Strong Multidisciplinary Integration: The agricultural ecosystem model constructed in the research comprehensively covers producers, consumers, and decomposers. It also incorporates factors such as human intervention and periodic changes, fully presenting the entire process from deforestation to the transformation of organic agriculture.

Combination of simulation and ablation experiment: By setting up different scenarios such as discontinuing the use of chemical agents, the impacts of various factors on the entire ecosystem and its components are clearly quantified. The practical suggestions drawn based on the detailed simulation results are highly reliable and can provide practical guidance for agricultural practices.

Lack of real data validation: This paper is mainly based on theoretical modeling, still a lack of effective verification with actual data. Whether it can accurately reflect the real situation of the real-world agricultural ecosystem remains to be further studied.

References

- [1] Fyfe, R. M., Woodbridge, J., & Roberts, N. (2015). From forest to farmland: pollen - inferred land cover change across Europe using the pseudobiomization approach. *Global change biology*, 21(3), 1197-1212.
- [2] Cardinale, B. J., Duffy, J. E., Gonzalez, A., Hooper, D. U., Perrings, C., Venail, P., ... & Naeem, S. (2012). Biodiversity loss and its impact on humanity. *Nature*, 486(7401), 59-67.
- [3] Godefroid, S., Piazza, C., Rossi, G., Buord, S., Stevens, A. D., Aguraiuja, R., ... & Vanderborght, T. (2011). How successful are plant species reintroductions?. *Biological conservation*, 144(2), 672-682.
- [4] Pretty, J., Benton, T. G., Bharucha, Z. P., Dicks, L. V., Flora, C. B., Godfray, H. C. J., ... & Wratten, S. (2018). Global assessment of agricultural system redesign for sustainable intensification. *Nature Sustainability*, 1(8), 441-446.
- [5] Matsuda, H., Ogita, N., Sasaki, A., & Satō, K. (1992). Statistical mechanics of population: the lattice Lotka-Volterra model. *Progress of theoretical Physics*, 88(6), 1035-1049.
- [6] Holling, C. S. (1959). The components of predation as revealed by a study of small-mammal predation of the European Pine Sawfly1. *The canadian entomologist*, 91(5), 293-320.
- [7] F. A. P. C. Gobas (2008). Food-Web Bioaccumulation Models. *Encyclopedia of Ecology*, 2, 1643-1652.